Crystalline Textures on the Al-Ni-Co Quasicrystal Surface

Mehmet ERBUDAK, Jean-Nicolas LONGCHAMP, Yves WEISSKOPF
Laboratorium für Festkörperphysik, ETHZ
8093 Zurich, SWITZERLAND

Abstract

We have generated cubic Al alloys as commensurate single crystals on the tenfold-symmetry surface of the quasicrystalline Al-Ni-Co alloy by ion bombarding its surface. We find that the crystal-quasicrystal interface contains several alignments of mutual high-symmetry directions and planes.

In order to explore the structural matching conditions at the crystal-quasicrystal interface, we have grown Al films on the decagonal surface of Al-Ni-Co by vapor deposition. The initial growth mode of Al is commensurate. As the coverage is increased, Al starts to grow in cubic textures breaking into multi-twinned, few-nanometer-large domains. The symmetry of the substrate determines thereby the orientation of the domains, while the degree of structural mismatch between the crystal and the quasicrystal limits the domain size.

Key Words: crystal, quasicrystal, interface, size selection, self assembly, epitaxy, quantum dots.

1. Introduction

An interface formed by two materials with dissimilar atomic structures cannot maintain conditions for epitaxial growth on a global scale. Locally, however, commensurability may persist on nanometer scale which leads to growth of self-size-selected monocrystalline domains [1]. Such nanometric configurations may find application as quantum-dot structures if, additionally, particular electronic conditions are fulfilled.

Periodicity is a unique characteristic of crystalline matter. Quasicrystals lack periodicity, but possess long-range orientational order with, *e.g.*, fivefold or tenfold point-group symmetries that cannot occur in ordinary crystals [2]. Therefore, the structural transition on the atomic scale at the interface where an ordinary crystal and a quasicrystal intersect is of particular interest. Below, we will outline two cases: In the first, the decagonal surface of $Al_{70}Ni_{15}Co_{15}$ (Al-Ni-Co) is physico-chemically modified by Ar^+ bombardment so that the thermodynamic conditions of stability for the quasicrystalline structure are not valid anymore. Instead, a CsCl-type cubic $Al_{50}(NiCo)_{50}$ alloy is established at the surface. The morphology consists of nanometric crystallites, exposing their (110) face, all oriented predominantly in the same direction with the alignment of some high-symmetry features in common with the substrate. Epitaxial growth conditions, like lattice and chemical matching observed in crystals, are apparently satisfied in this case on a local scale. In the second case, we vacuum deposit Al onto the quasicrystalline surface and observe the growth of several Al domains in the native face-centered cubic (fcc) structure, each aligned with the (111) surface parallel to the decagonal face and in 10 azimuthal increments producing a pseudo-decagonal symmetry.

While recognizing the potential use of the crystal-quasicrystal epitaxy in producing quantum dots in the low-nanometer dimensions, we attempt to extract average structural information about the quasicrystal by observing the local alignment of the cubic structure on its surface. Such information has remained concealed so far. This report is organized as follows: relevant experimental details are conveyed in the second section.

In the third section, results on Ar^+-bombardment induced structures as well as observations due to Al deposition are reported. In the discussion and conclusions section, some considerations on the decagonal surface structure with respect to the cubic overlayer are presented.

2.   Experimental

We consider here the decagonal quasicrystal Al-Ni-Co, which is quasiperiodic in two dimensions and periodic in the third dimension, the tenfold-symmetry axis. The two-layer periodicity is 0.408 nm [3]. The tenfold-symmetry surface, due to its flatness, is well suited as a substrate to grow a crystalline structure by vapor deposition.

A sample with dimensions $5 \times 3 \times 1$ mm^3 was oriented by means of the x-ray Laue method with an accuracy of $\pm 0.5°$ along the decagonal symmetry axis, cut, and polished mechanically to an optical finish [4]. The quasicrystalline surface was cleaned in ultrahigh vacuum in the lower 10^{-8}-Pa region by cycles of heat treatment (700 K for 30 minutes) and sputtering with Ar^+ ions (1.5 keV, 4.5×10^{-7} A/mm^2).

The atomic structure and the structural quality of the investigated surface were determined by low-energy electron diffraction (LEED). Diffraction spots are generated by directing a monochromatic beam of electrons in the energy range of $30 - 300$ eV onto the specimen surface and recording the backscattered electrons. The result is a projection of the surface atomic distribution into reciprocal space, while the size and symmetry of a region of coherence is conserved. In LEED experiments, quantitative real-space information about the atomic structure can be deduced from the position of Bragg spots and the energy dependence of their intensities. The size of diffraction spots are used to extract information about the extent of the region on the surface that contributes coherently to pattern formation [5].
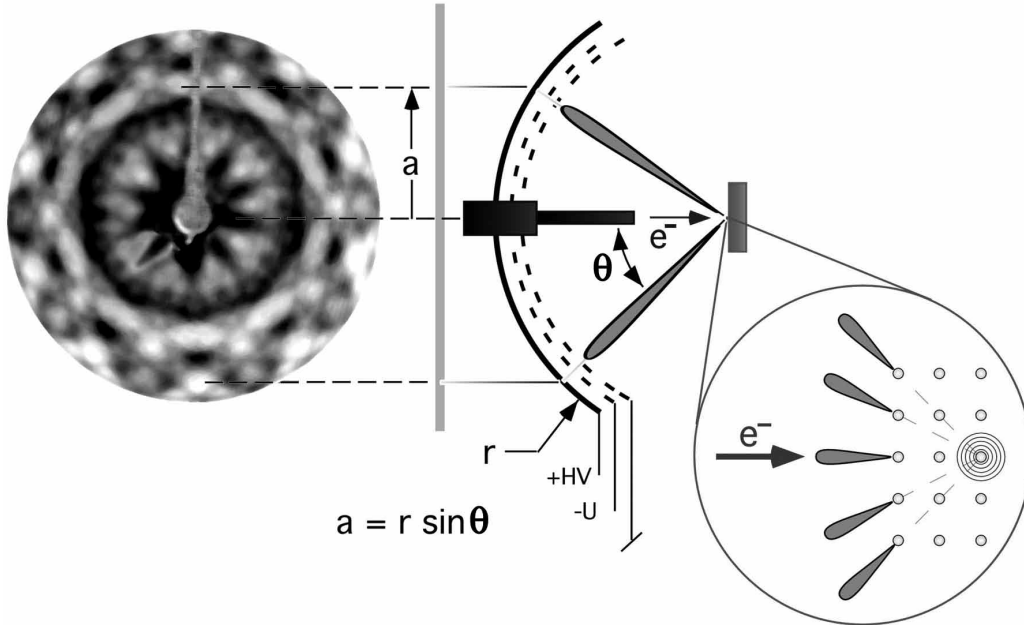
Figure 1. Schematic representation of the LEED/SEI experiment and the image formation in SEI. An electron gun is placed along a central axis of the spherical display unit, which consists of two grids and a see-through display unit. The sample is located at the center of the sphere. The circular inset illustrates the forward-focusing effect responsible for image formation in SEI.

The secondary-electron imaging (SEI) technique [6] was performed to examine the local atomic order in the near-surface region in *real space*. SEI involves the excitation of the surface region by electrons having an energy near 2 keV and subsequent two-dimensional spherical recording of the backscattered electrons. At energies of several keV, elastic forward scattering is the dominant process. The secondary electrons

that can escape the solid are predominantly those scattered by atoms near the source. These electrons produce bright spots on the collector screen for particular directions, defined by the source and the adjacent atoms. Consequently, the observed pattern represents a central projection of the average real-space atomic arrangement around each source, with many sources contributing incoherently to the pattern. Hence, the atom arrangement of the structure producing the SEI pattern must not necessarily possess translational long-range order; it only has to have its atoms in an equal local environment. The experiment, including the excitation and emission processes, is schematically shown in figure 1. Also displayed is a pattern with tenfold symmetry. Beside revealing dense atomic rows at and below the surface, SEI patterns also display so-called Kikuchi bands, which originate from Bragg diffraction of quasielastically scattered electrons at parallel planes of high atomic density [7].

The combination of SEI with LEED offers the possibility of studying the orientation of the top surface layers with respect to the bulk, while comparing local and global structural features. LEED and SEI use the same apparatus, and a secondary-electron image is obtained by simply increasing the electron energy to 2 keV.

Chemical information about a near-surface region of the specimen is obtained by Auger electron spectroscopy (AES). In AES, the radiationless recombination of inner shells, excited by an electron beam of $2 - 3$ keV energy, is recorded as a function of the electron energy. Secondary electrons with the energy of Auger transitions are characteristic of the elements found near the surface, while the electron intensity represents their concentration.

Al was evaporated from a power-regulated, home-made atomic-beam source. The evaporation rate was 0.08 ± 0.01 nm/min, calibrated using AES signals. During the Al deposition the substrate temperature was held at 300 K. Some experimental details have been communicated earlier [8].

3.   Results

3.1.   Physico-chemically induced cubic domains

Figure 2a shows an SEI pattern from the quasicrystalline Al-Ni-Co sample for which the tenfold-symmetry axis coincides with the surface normal. This was also the incident direction of the primary-electron beam. The rim of the collector screen represents the polar angle $\theta = 52\pm1°$. Scanning the electron beam across the sample surface left the pattern unchanged confirming that the specimen consisted of one single grain. The overall decagonal symmetry is the most striking feature observed in the pattern. Significant contribution to the pattern originates from Kikuchi bands due to planes inclined by $\theta = 30 \pm 2°$ from the decagonal direction. Bright patches of increased electron intensity appear on concentric rings at different polar angles. Features on the innermost ring occur at $\theta = 18 \pm 2°$. A concentration of bright spots, which are arranged in decagonal symmetry, is located at $\theta = 35 \pm 2°$. Between these two rings of bright patches, a dark circular area with no significant electron intensity is observed at $\theta = 25 \pm 2°$ suggesting a tube-like hollow structure along the decagonal axis. Near the edge of the pattern, additional bright patches are observed which are distributed also in decagonal symmetry.

Since a direct projection imaging of the vectors connecting the next-neighbor atoms with a reference atom is responsible for the formation of the pattern, its computational interpretation using a simple geometric analysis is straightforward. Thus, a structure model has been found consisting of coaxial stacking of equal-sized alternating pentagons, each rotated by $36°$ with respect to the next layer [9]. This so-called pentagonal antiprism is, in principle, the characteristic feature for several quasicrystalline structure models [2]. This simple model can accurately reproduce the major symmetry elements of the experimental pattern if the interlayer distance, h, is set equal to the center-to-corner distance of the pentagons. According to x-ray diffraction results, $h = 0.408/2$ nm [3] which results in an interatomic distance of $a = 2h \sin 36° = 0.2398$ nm. This value is within 1.4% of 0.2431 nm, the nearest-neighbor distance in Al-Ni-Co [10].

Figure 2b presents an SEI pattern obtained from Al-Ni-Co with the electron beam directed normal to the surface. However, the sample had previously been sputtered for 30 minutes with Ar^+ ions at normal incidence. There are some features with decagonal symmetry located on a small circle with an opening angle of $\theta = 18°$. Other features of the pattern show precise *orthogonal* symmetry which can be interpreted by a direct projection of the vectors in a hemisphere connecting the nearest-neighbor atoms to a reference atom

in a body-centered cubic (bcc) structure with the [110] direction oriented normal to the surface. Then, the two bright patches, which lie approximately 71° apart at the top and bottom of the pattern, represent the [11$\bar{1}$] and [111] directions, respectively. The [010] (left) and the [100] (right) directions are separated by 90°. We recognize the [00$\bar{1}$] and [1$\bar{1}$0] directions lying in the surface and perpendicular to the surface normal [110]. On this figure, four crystallographic planes, (011), (101), ($\bar{1}$01), and (0$\bar{1}$1) are also marked.
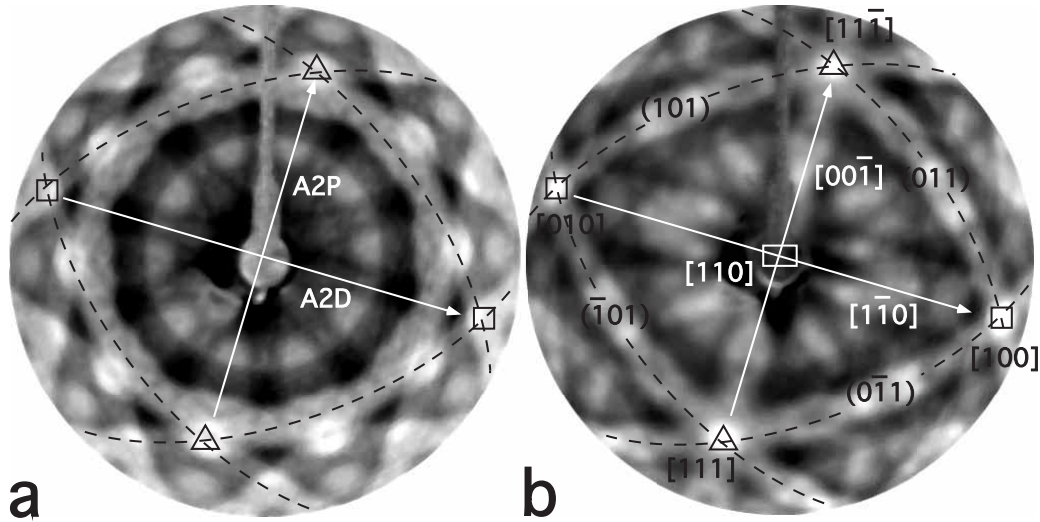

Figure 2. Secondary-electron patterns obtained at 2 keV from a) the well-ordered decagonal surface of Al-Ni-Co and b) the same quasicrystal after bombarding its surface with Ar$^+$ ions. High-symmetry features are marked on the pattern. The white arrows denote directions lying in the sample surfaces. [110] is normal to the surface and parallel to the decagonal direction.

Beneath the top few atomic layers imaged by SEI the quasicrystalline structure is still perfectly intact, which was established by reflection x-ray Laue diffraction. This means that the specimen is a bulk decagonal quasicrystal covered with a layer of bcc units, all of which must possess the identical orientation to generate the SEI pattern shown in Fig. 2b. The thickness of the bcc layer may be as thick as $3-14$ nm [11]. The lower limit, however, corresponds to the information depth of SEI, which is of the order of $2-3$ nm [12]. This layer is still thin enough to transmit the decagonal features observed at 18° which originate from the bulk quasicrystalline structure. Interestingly, AES measurements revealed a surface composition of Al$_{50}$(NiCo)$_{50}$, *i.e.*, there is a strong depletion of Al in a near-surface region caused by preferential sputtering. In fact, AlNi, AlCo, and Al$_2$NiCo are all well-known to have the CsCl structure with a lattice constant of $0.28-0.29$ nm [13]. This is consistent with our observations, because SEI cannot differentiate the different atoms and can therefore not distinguish between bcc and CsCl structures.

On the SEI pattern shown in Fig. 2b, several crystallographic features are marked. The [110] direction, which coincides with the surface normal, is concealed behind the shadow of the electron gun. In order to investigate the orientational relationship between the decagonal structure of the quasicrystalline surface and the cubic units on the Ar$^+$-bombarded surface, we superpose the crystallographic directions onto the pattern shown in Fig. 2a. The [110] axis is clearly oriented parallel to the tenfold-symmetry direction. We find that the ⟨111⟩ axes coincide with the quasicrystalline features observed at $\theta = 35 \pm 2°$ within the experimental accuracy. Similarly, ⟨100⟩ axes overlap with electron intensities observed for the quasicrystal as intersections of the planar structures. Four of these planes are indicated by dashed lines, which coincide with (011), (101), ($\bar{1}$01), and (0$\bar{1}$1) crystal planes. There are two kinds twofold-symmetry axes of the quasicrystalline structure, denoted A2D and A2P [14], which lie in the decagonal plane of the quasicrystal. We note that the A2P direction is parallel to the [00$\bar{1}$] axis and the A2D direction is parallel to [1$\bar{1}$0]. While this correspondence is accurate within experimental error, there is another match between A2D and the surface ⟨111⟩ directions within ±1°.

The almost perfect overlap of several high-symmetry features illustrated in Figs. 2a and 2b is a signature of the satisfactory structural agreement between the cubic phase and the decagonal surface at the interface. This observation implies that at this interface these two phases become indistinguishable on local scale. It is very interesting that the cubic structure develops in *one* particular direction and not in all *five* equivalent directions. Apparently, there is a preferential direction on the quasicrystalline surface maybe induced by preferred orientation of steps influencing the nucleation behavior of surface species.
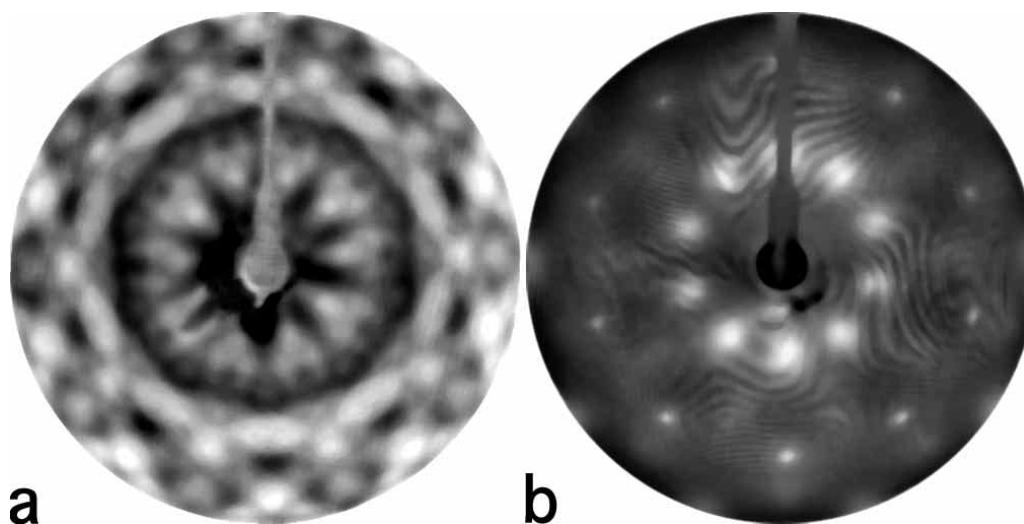
Figure 3. a) SEI and b) LEED patterns obtained from the surface in the intermediate phase. The latter is obtained at $104\,$eV.

It has been observed that the surface composition is recovered when the specimen is heat treated at $700\,$K. This transition occurs because the kinetics of segregation leads to an equilibrium concentration of Al at the surface which apparently prefers the assembly of the thermodynamically stable quasicrystalline phase at this temperature [15, 16]. There is, however, an intermediate phase reached at annealing temperatures around $365\,$K. Figure 3a illustrates an SEI pattern obtained from the surface at this stage which resembles that from the quasicrystalline sample shown in Fig. 2a. We notice that decagonal features up to $\theta \approx 30°$ appear fuzzier for this intermediate surface. Furthermore, the pattern for this phase contains 10 additional distinct spots at $\theta = 45°$. LEED is performed on this surface in order to identify the surface structure. Although no diffraction is observed due to the lack of constructive interference from the mono-oriented CsCl surface structure, LEED patterns have been obtained from the intermediate phase. One such pattern is shown in Fig. 3b which shows a rotational tenfold symmetry. Applying Bragg's law to this and other patterns obtained at other energies, we calculate 0.229, 0.290, and $0.401\,$nm as the distances of parallel rows of surface atoms, within our experimental accuracy. If we take the lattice parameter $a = 0.2874\,$nm of $Al_{50}(NiCo)_{50}$ [13], parallel rows of scatterers on the (110) surface are found at $a \times 2/\sqrt{6} = 0.2347\,$nm, $a = 0.2874\,$nm, and $a \times \sqrt{2} = 0.4064\,$nm in agreement with the experimental values. Consequently, the LEED experiments have helped us identify that the intermediate phase consists of 5 CsCl domains exposing their (110) surfaces, aligned in equal azimuthal distribution. This analysis implies that the 10 additional spots at $\theta = 45°$ observed in the SEI pattern presented in Fig. 3a are due to the $\langle 100 \rangle$ axes of the cubic surface textures oriented with their [110] directions parallel to the surface normal. One of these five domains corresponds to the surface phase presented in Fig. 2b. AES measurements of this intermediate surface structure result in a surface stoichiometry of $Al_{56}Ni_{22}Co_{22}$.

The profiles of the diffraction spots observed from the intermediate stage show an energy-dependent modulation. This is typical of surface defects, *e.g.*, limited spatial extent of the single-crystalline domain regions on the surface [5]. The angular width of a diffraction spot is negligibly small for a perfect crystalline surface and perfect experimental conditions. The halfangle ϵ of a spot is approximately given by

$$\epsilon = \lambda/(2Ma\cos\theta), \tag{1}$$

where λ is the electron wavelength and Ma the size of the coherence region on the surface, both in the same length units [17]. The finite size of the spots, which appear around $\theta = 20°$ in Fig. 3b, yields a region of coherence on the surface, which has a size of 1 ± 0.2 nm. The other set of 10 spots lying on a polar circle of $\theta \approx 45°$ point to an island size of about 3.5 nm.

The quasicrystalline surface can be recovered gradually upon annealing the sample for approximately 90 minutes at 700 K. The sputtering-annealing cycle can be repeated reproducibly and at will, indicating that the quasicrystalline phase is the thermodynamically stable one. The transformation to the quasicrystalline phase is limited by the kinetics of diffusion and re-assembly of the stable structure. Whenever the chemical conditions are satisfied, this transformation, *i.e.*, formation of the quasicrystalline phase starting from an appropriate cubic seed, is highly favorable. Hence, the bcc structure seems to be a *progenitor* of the quasicrystalline phase [18].

3.2. Surface textures produced by vapor deposition

Figure 4a depicts a LEED pattern obtained from the clean decagonal surface at an electron energy of 55 eV. The occurence of sharp diffraction spots points to an orientational long-range order in decagonal symmetry. During the initial stage of Al growth up to about 1 atomic layer (AL), corresponding to about 0.23 nm, we first observe no change and then a decrease in the diffraction intensities from the quasicrystalline substrate without any indication of additional spots due to the evolution of a new surface structure. Electron scattering at Al atoms is incoherent with the scattering at the substrate atoms. This observation points to an unordered and incommensurate distribution of Al at the surface, *i.e.*, Al neither fits into the decagonal matrix nor forms fcc structure.

The kinetic energy of $L_{2,3}VV$ Auger transitions in Al depends on the electronic state of Al atoms. The transition from the quasicrystalline to the metallic environment results in a shift to higher energies. By measuring this shift in the AES signal during Al deposition we find that already 0.5 AL thick Al is metallic, *i.e.*, Al atoms are predominantly bound in the Al matrix instead of the quasicrystalline Al-Ni-Co alloy. This observation shows that even for a submonolayer coverage Al does not participate in chemical bonding with the quasicrystalline substrate. On the other hand, the amount of Al is apparently too low to establish a crystalline order at this stage and assumes instead energetically favorable quasicrystalline sites.

After depositing 0.4-nm Al, new LEED spots appear, while several spots from the underlying quasicrystalline substrate are still visible. Figure 4b shows a LEED pattern at 55 eV from the surface with 0.6-nm thick Al overlayer. The pattern consists of thirty diffuse spots lying on a circle. The diffraction spots indicate that the Al film has the same rotational order as the quasicrystalline substrate. These patches assume their final shape not until more than about 1 nm of Al are deposited. The fact that the substrate is still detectable for higher film thicknesses confirms a three-dimensional growth mode.

The comparison of the LEED patterns shown in Figs. 4a and 4b indicates that the underlying substrate acts as a symmetry template for the orientation of the Al domains. The rotational alignment is best documented by the ten faint spots due to the substrate occurring near the rim of the screen. They are still detectable in the pattern from the sample with 0.6-nm thick Al overlayer. Using Bragg's law for the diffraction spots in Fig. 4b, we obtain approximately $d_1' = 0.146$ nm and $d_2' = 0.250$ nm for the distances between parallel rows of scatterers. These distances and the relative positions of the diffraction spots confirm the formation of Al fcc domains exposing the (111) surface.

Analyses of the LEED spot profiles lead to valuable information on the quality of the surface structure. Using Eqn. (1) we find a domain size of 3 nm. A closer inspection reveals, that the spots are twinned in azimuth by about 2° [19]. Resorting to SEI observations, we realize that there are two sets of 10 3-nm large fcc domains at the surface in registry with the decagonal substrate, each twinned by approximately 2°. The domains within each set are distributed in azimuthal increments of 36°. This growth mode in the form of domains having the bulk fcc structure persists even for thicker films.
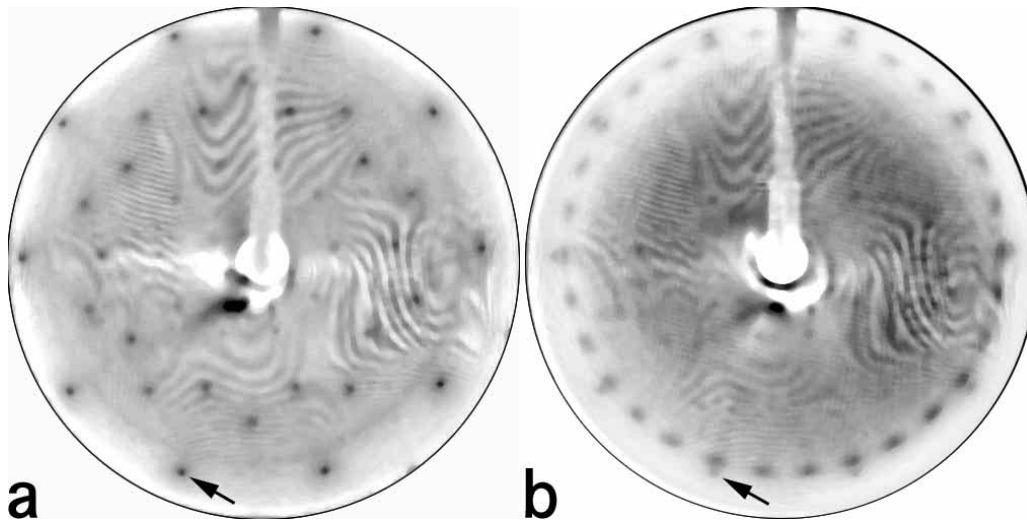
Figure 4. LEED patterns at normal incidence and a primary-electron energy of 55 eV from a) the clean decagonal surface of Al-Ni-Co and b) after depositing 0.6-nm thick Al. The arrows point to the same diffraction spot originating from the decagonal substrate. The patterns are grey-scale inverted for better identification of diffraction features.

4. Discussion and Conclusions

We have generated cubic crystalline domains on the decagonal surface of the two-dimensional quasicrystal Al-Ni-Co by bombarding with Ar^+ ions at $1.5\,keV$. The structure and the stoichiometry of the surface layer indicates the formation of $Al_{50}(NiCo)_{50}$ crystallites with a thickness of $2-3\,nm$, estimated using the information depth of the SEI experiment. The domains are oriented all in one particular direction well aligned with one high-symmetry direction of the quasicrystalline surface. The correspondence of the symmetry features in the decagonal and cubic structure is remarkable. Well-defined SEI patterns are observed from the surface in the absence of diffraction. Successful imaging of the surface using SEI implies the existence of perfect orientational order in these layers, while the absence of electron diffraction indicates that the surface consists of small islands without translational long-range order. This can be attributed to the remaining mismatch between crystal and quasicrystal, which causes strains in the cubic phase and prevents the growth of a long-range ordered surface layer. Thus, each separate island contributing to image formation in SEI is not sufficiently large to generate discernible LEED patterns. Yet, it is equally realistic to imagine a cubic near-surface region of the quasicrystal, which is covered by a 1- or 2-atoms thick disordered layer, which prevents formation of diffraction for the scattered electrons.

It is puzzling that the crystalline material in the near-surface region has a preferred orientation with respect to the decagonal quasicrystalline surface. The decagonal structure is a suitable template with fivefold or tenfold atomic symmetry. Therefore, one would expect a corresponding occurrence of differently oriented crystallites. We repeatedly observe, however, one and only one single alignment. There are several plausible, but not exclusively convincing arguments for this observation [9], one of which is mentioned above.

The crystalline layer at the surface is metastable. A mild heat treatment of the sample induces the formation of 5 different domains each aligned along a particular direction of the quasicrystalline surface. The assembly of these domains occurs all the way to the surface as deduced from the observation of diffraction patterns. The spot intensities, however, are not ideally shaped and present an energy-dependent behavior. The data allow us to estimate that the surface consists of crystalline domains with a size distribution of approximately $1-3.5\,nm$.

The interface formed by the quasicrystal and the cubic structure deserves attention. The nearest-neighbor distance in the quasicrystal is $a_1 = 0.2431\,nm$ corresponding to Al-Ni and Al-Co bond lengths. This can be extracted from the quasilattice constant $a = 0.3757\,nm$ [10] by using $a_1 = 2/5\,\tau\,a$, where $\tau = (\sqrt{5}+1)/2$ is the golden mean. The second nearest-neighbor distance is $a_2 = 0.2858\,nm$ corresponding to Al-Al bonds

[20]. The CsCl structure exposing its (110) surface with a lattice parameter $b = 0.2874\,\mathrm{nm}$ for $\mathrm{Al}_{50}(\mathrm{NiCo})_{50}$ [13] has a nearest-neighbor distance of $b \times \sqrt{3}/2 = 0.2489\,\mathrm{nm}$. We find that the lattice mismatch along the cubic $[00\bar{1}]$ direction is about 2% ($3b = 0.8622\,\mathrm{nm}$ compared to $2a_1 \times (1 + \tau/2) = 0.8795\,\mathrm{nm}$). Along the $[1\bar{1}0]$ direction, the mismatch is only 0.3% ($3\sqrt{2}b = 0.12192\,\mathrm{nm}$ compared to $5a_1 = 0.12155\,\mathrm{nm}$). These considerations show that, if appropriately aligned, small crystallites can grow at favorable adsorption sites on the quasicrystalline substrate. A model for this interface [19] was recently realized by using the atom coordinates of a realistic decagonal surface [21].

Strain between the incommensurate lattices prevents the growth of a crystalline surface structure. Subsequent annealing leads to the formation of 5 domains of bcc structure rotated by 72° relative to each other. The annealing process makes Al atoms segregate towards the surface and release some of the existing strain, resulting in a more ordered phase.

We have evaporated Al on Al-Ni-Co, because Al is a good candidate to grow in quasicrystalline structure due to its high affinity to this alloy. Clearly, the chemical and structural constraints are not sufficiently effective to make Al grow in quasicrystalline order. For few-monolayers thicknesses, we could not discern any order in the film. Interestingly, above half-a-monolayer coverage, a distinct metallic character of the Al film sets in. With increasing thickness, the Al film gradually develops the native fcc structure, in nano-sized domains, with their densest packed and therefore energetically most favorable (111) surfaces oriented parallel to the substrate decagonal surface. A total of two sets of 10 distinct in-plane orientations of these domains are observed. Analysis of the LEED spot profiles indicates that the domains have almost a circular shape with a diameter of about 3 nm. The tenfold-symmetric quasicrystalline substrate clearly acts as an effective template and imposes the alignment of the Al domains in tenfold symmetry. We conjecture that there are some energetically favored positions on the decagonal surface for the nucleation and growth of the Al islands. Since these minimum-energy sites are part of the surface structure, they are distributed in an aperiodic order on the decagonal surface. Therefore, it is necessary to conclude that the 3-nm large Al islands themselves are assembled on the surface in a quasiperiodic order. The resulting structure is a novel quasicrystal with a base consisting of nano-sized Al crystallites distributed in a decagonal quasicrystalline matrix.

Acknowledgements

References

[1] J. R. Arthur, *Surf. Sci.*, **500**, (2002), 189.

[2] C. Janot, Quasicrystals, A Primar (Clarendon, Oxford. 1992).

[3] W. Steurer, T. Haibach, B. Zhang, S. Kek and R. Lück, *Acta Cryst. B*, **49**, (1993), 661.

[4] A. R. Kortan, F. A. Thiel, H. S. Chen, A. P. Tsai, A. Inoue and T. Masumoto, *Phys. Rev. B*, **40**, (1989), 9397.

[5] M. Henzler, *Surf. Sci.*, **19**, (1970), 159.

[6] M. Erbudak, M. Hochstrasser, E. Wetli and M. Zurkirch, *Surf. Rev. Lett.*, **4**, (1997), 179.

[7] K. Z. Baba-Kishi, *J. Mater. Sci.*, **37**, (2002), 1715.

[8] M. Erbudak, T. Flückiger, A. R. Kortan and R. Lüscher, *Prog. Surf. Sci.*, **75**, (2004), 161.

[9] B. Bolliger, M. Erbudak, M. Hochstrasser, A. R. Kortan and M. Zurkirch, *Phys. Rev. B*, **54**, (1996), R15 598.

[10] W. Steurer and A. Cervellino, *Acta Crystallogr. Sec. A*, **57**, (2001), 333.

[11] T. Flückiger *et al.*, *Surf. Interface Anal.*, **34**, (2002), 441.

[12] J. C. Ashley and C. J. Tung, *Surf. Interface Anal.*, **4**, (1982), 52; S. Tanuma, C. J. Powell and D. R. Penn, *Surf. Interface Anal.*, **17**, (1991), 911.

[13] P. Villars and L. D. Calvert, Pearson's Handbook of Crystallographic Data for Intermetallic Phases (ASM International, Ohio. 1991).

[14] Y. Qin, R. Wang, Q. Wang, Y. Zhang and C. Pan, *Philos. Mag. Lett.*, **71**, (1995), 83.

[15] M. Zurkirch, B. Bolliger, M. Erbudak and A. R. Kortan, *Phys. Rev. B*, **58**, (1998) 14 113.

[16] T. Flückiger, PhD Thesis, Department of Physics, ETH Zürich, Switzerland, 2003; http://e-collection.ethbib.ethz.ch/cgi-bin/show.pl?type=diss&nr=15308.

[17] A. Guinier, X-Ray Diffraction in Crystals (Freeman, San Francisco. 1963).

[18] V. E. Dmitrienko and S. B. Astaf'ev, *Phys. Rev. Lett.*, **75**, (1995), 1538.

[19] T. Flückiger, Y. Weisskopf, M. Erbudak, R. Lüscher and A. R. Kortan, *Nano Lett.*, **3**, (2003), 1717.

[20] M. Michalkovič *et al.*, *Phys. Rev. B*, **65**, (2002), 10 4205.

[21] K. Saitoh, K. Tsuda and M. Tanaka, *J. Phys. Soc. Jpn.*, **67**, (1998), 2578.